IMPACT TOLERANCE OF CERAMIC MATRIX COMPOSITES FOR AEROSPACE APPLICATIONS

Gerardus Janszen[1], Antonio Maria Caporale[1], Lorenzo Cavalli[2], Mario De Stefano Fumo[3] & Alessandro Airoldi[1]

[1]Aerospace science and technology department, Politecnico di Milano, Via La Masa 34, 20154, Milan, Italy
[2]Petroceramics S.p.A., Viale Europa, 2, 24040 Stezzano (BG), Italy
[3]Centro Italiano di Ricerche Aerospaziali, Via Maiorise, 81043 Capua (CE), Italy

Abstract

Ceramic Matrix Composites (CMCs) guarantee the right balance of stiffness, strength, temperature and oxidation resistance to be the best choice for hot structure of reusable space vehicles. Nowadays specific design approach for aerospace CMCs are not fully developed. The aim of this study is to define a methodological procedure to assess the damage tolerance of a C/SiC CMC in the case of low-energy impacts. For this reason, in the first part of this work, a low-energy impact testing campaign was performed on beam and plate specimens with the aim of determine the threshold energy that causes a Barely Visible Impact Damage (BVID), which is a damage that is hardly detectable during the inspections. In the second part of the work, the effectiveness of different tests in evaluating the specimen's residual strength was assessed. Firstly, Compression After Impact (CAI) test was tried, showing that it is not effective on CMCs, which are stiff and particularly resistant to compression. Then, flexural testing was tried, first on specimens cut out from the panels, then on the entire panels. A Computed Tomography (CT) scan was performed on the cut-out specimens showing the presence of delaminations through the thickness of a specimen with a BVID. The three-point bending test on these specimens showed noticeable reduction of strength but only in the region close to the impact point. A three-point bending test was then performed on two plate specimens, one as-built and one with a BVID. Particular attention was given in evaluating the effect of anticlastic curvature in creating unwanted stress concentrations. The results showed a reduction of about 25% of the flexural strength of the impacted panel. Concluding, an experimental protocol was presented and validated to determine the damage tolerance of C/SiC panels in the presence of low-energy impact damages.

Keywords: Impact testing, Ceramic Matrix Composite, Damage Tolerance, Reusable Space Vehicles

1. Introduction

Ceramic Matrix Composites (CMCs) are a relatively new class of materials, which development started back in the 1960 [1]. They are ceramic materials, reinforced with particles, short or continuous fibers. Their superior resistance to temperature and oxidation, and their superior tribological properties, make them appealing for a wide range of applications. Graphite, silicon carbide and oxides are the most used materials as a matrix for CMCs, depending on the application. Carbon fibers, SiC fibers, and oxide fibers are the most common type of reinforcement. Their development started to deal with the thermal shock in the ceramic tiles used as Thermal Protection Systems (TPSs) of re-entry space vehicles, with the aim of increasing their fracture toughness. From the space field, the application of CMCs rapidly spread to the automotive and aeronautical industry, in which they are widely used for braking systems, and more recently in aeronautical engine components. Among the CMCs, carbon fiber reinforced SiC, referred to as C/SiC, showed to be the best tradeoff among mechanical and thermal properties, manufacturability, and costs. Different manufacturing techniques exist for this material, such as Chemical Vapor Infiltration (CVI), Polymer Infiltration and Pyrolysis (PIP), and Liquid Silicon Infiltration (LSI). This last technique consists of the pyrolysis of a carbon fiber reinforced phenolic preform, followed by the infiltration of liquid silicon, which reacts with the carbonaceous residual of the phenolic resin to form SiC.

During the Space Shuttle Program, reinforced Carbon/Carbon (RCC) used as thermal-shock resistant TPS, proved to be one of the keys of the reusability of the vehicles. In recent years, progress in CMCs industry promoted a renewed interest on Reusable Space Vehicles (RSVs) which could significantly reduce the costs of the access to space. For this reason, the development of design procedures specific for CMCs are of extreme interest. After 1970, a new design philosophy called “damage tolerance” was established in the aeronautical field in which the constant necessity of weight reduction does not allow large design safety factors. By definition [2], a damage tolerant structure must be able to withstand damages, developed in any moment of the life of the component, and their evolution for a time long enough to guarantee its detection. Thus, a deep knowledge of the typical damages, as well as of their evolution, is necessary, together with an adequate maintenance schedule. Low energy impacts, caused by hail or a falling tool for example, are the typical events that can cause hardly detectable damage, such as a delamination inside an impacted panel, which presence and evolution must be considered. Barely Visible Impact Damage (BVID) is then defined as that damage which cannot be easily detected by the routinary visual inspection, but only using more advanced techniques that could require the disassembly of the vehicle parts.

This work is a methodological study to propose and assess the effectiveness of an experimental procedure to evaluate the resistance of C/SiC structures to low energy impacts following a damage tolerant philosophy. The material used is a SIC matrix reinforced with fabrics of carbon fibers. It is produced by Liquid Silicon Infiltration (LSI) [3], [4], [5], [6], a technique in which molten silicon is infiltrated in the pyrolyzed preform by means of capillarity. The experimental procedure must include an impact testing methodology to cause a BVID in the material and a second test to evaluate its residual properties. In previous literature works, this was achieved using tensile and compressive tests, methods which have a certain complexity [7], [8], [9]. Thus, a custom impact testing facility was developed and used on beam and plate C/SiC specimens to evaluate the BVID energy, as well as the typical morphology of an impact damage. Then, different methods to evaluate the residual properties of the specimens were assessed, considering the specific features of the material. Indeed, LSI C/SiC typically shows a certain amount of nonlinearity due to the presence of intense residual thermal stresses (RTS) [1], [10], [11], which are more visible in tension that in compression, in which the material shows a higher linearity and a higher strength.

2. Material and methods

A custom low-energy impact facility was built to test the C/SiC specimens. It consists of a polycarbonate (PC) tube with a diameter of about 40 mm, vertically fixed to a wall, in which the impactors were dropped. At the end of the tube, on the floor, the different specimens’ fixtures were placed. To avoid secondary impacts, the PC tube is tilted at an angle of 15° in the plane of the wall to which it is fixed. In this way, the impactor hits the specimens with a certain angle, and rebounds away. A picture of the testing setup is shown in Figure 1. The first kind of impactor used was steel bearing ball with different diameters. Then, to increase the impactor mass without modifying the setup, a rod-shaped impactor was built by soldering a steel bar to one of the previous bearing balls. A picture of the impactors is shown in Figure 1.

Figure 1: Low-energy impact experimental setup. Details of the polycarbonate tube equipped with photocells and the two types of impactors used, with their masses.

To have a reliable measurement of the impact energy, two photocells were mounted at the outlet of the tube, 10 mm apart. Their signal, acquired at 12.5 kHz, was used to determine the exit velocity of the impactors. At the same time, a high-speed camera was used to capture the images of the impact. It was placed on the floor, pointing normally to the wall to which the tube is fixed, and it was used to verify the accuracy of the impact.

A first preliminary study on the impact resistance of C/SiC was performed using beam specimens with dimensions $4\,mm\ \times 12\,mm \times 145\,mm$. Eight specimens with lamination sequence $[0]_{20}$, called C/SIC-B0 and six specimens with lamination sequence $[0/45/90/-45]_{5S}$ were tested, and their residual strength was assessed by means of a three-point bending test. In the fixture used, specimens were clamped at the ends, allowing deflection during impact. This configuration was chosen because it better represents a more critical condition compared to a fully supported one, in which the stress is mainly compressive. A picture of the fixture is shown in Figure 1-a.

A second study was performed using $150\,mm \times 100\,mm \times 4\,mm$ C/SiC plates with quasi-isotropic lamination sequence, $[0/45/90/-45]_{5S}$. This measures and the fixture were designed following the standard for low energy impact of CFRP plates [12]. A figure of the fixture is shown in Figure 1-b. The efficacy of different test in assessing the post-impact residual strength of the panels was then evaluated.

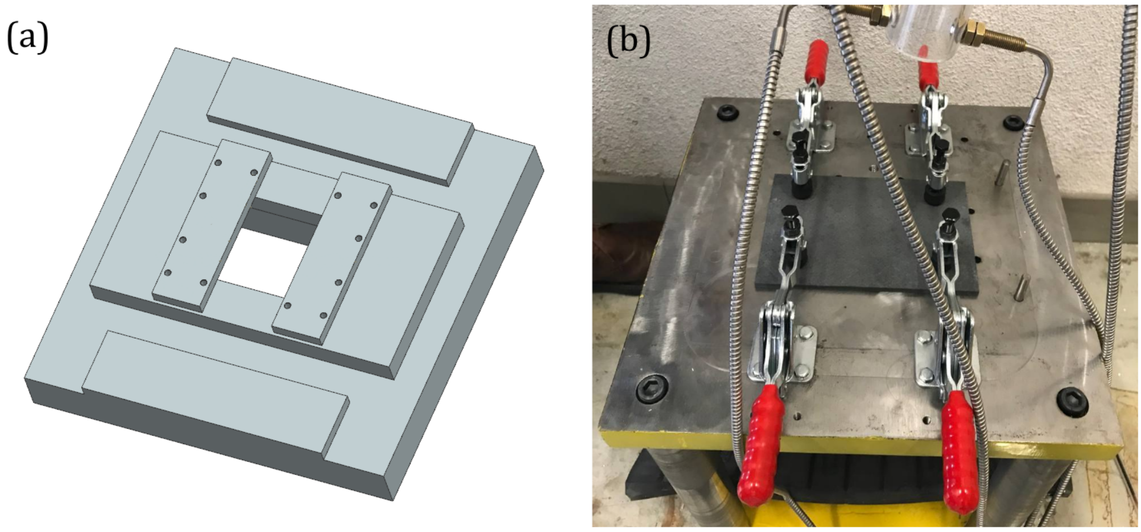

Figure 1: Fixture for low-energy impact test of (a) beam-shaped and (b) plate specimens.

3. Impact testing of C/SiC beams

The list of beam-shaped specimens impacted is presented in Table 1. Three different bearing balls with a mass of 12 *g*, 19 *g*, and 28 *g* were used, resulting in impact energies ranging from 0.2 *J* to 0.4 *J*. Four frames taken from the high-speed video recorded during an impact test are shown in Figure 2.

Table 1: List of beam-shaped C/SiC specimens subjected to low-energy impact.

Specimen	Impactor mass *g*	Impact energy *J*	Flexural test
C/SiC-B0-I1	12	0.208	yes
C/SiC-B0-I2	12	0.208	yes
C/SiC-B0-I3	12	0.208	yes
C/SiC-B0-I4	19	0.329	yes
C/SiC-B0-I5	19	0.293	yes
C/SiC-B0-I6	19	0.329	yes
C/SiC-B0-I7	28	0.401	No (broken during the impact)
C/SiC-B0-I8	19	0.274	yes
C/SiC-BQI-I1	12	0.208	yes
C/SiC-BQI-I2	12	0.208	yes
C/SiC-BQI-I3	19	0.329	yes
C/SiC-BQI-I4	19	0.329	yes
C/SiC-BQI-I5	28	0.482	yes
C/SiC-BQI-I6	19	0.329	yes

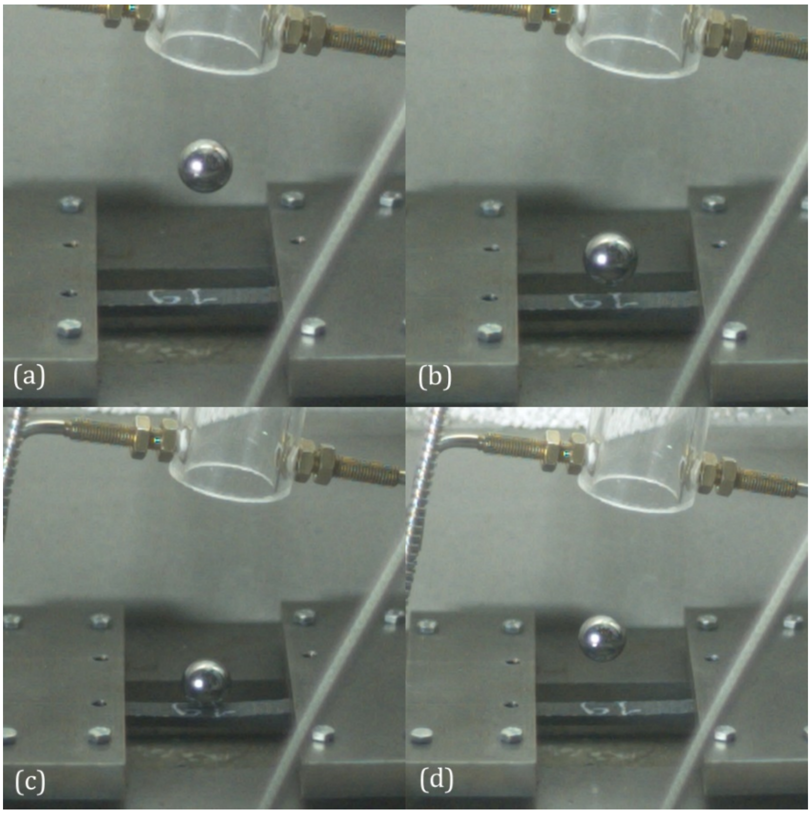

Figure 2: Frames from a high-speed video of a low-energy impact on a C/SiC beam specimen.

All the specimens impacted with an energy of $\sim 0.2\,J$ did not show any indentation or residual deflection. Increasing the energy up to $\sim 0.3\,J$, the specimens started to degrade. Typically, a fracture opened in the tensed face of the specimens, cracking the matrix, as shown in Figure 3. Moreover, fibers bridging was observed in the cracks, avoiding the global failure of the specimens, which retained a certain resistance.

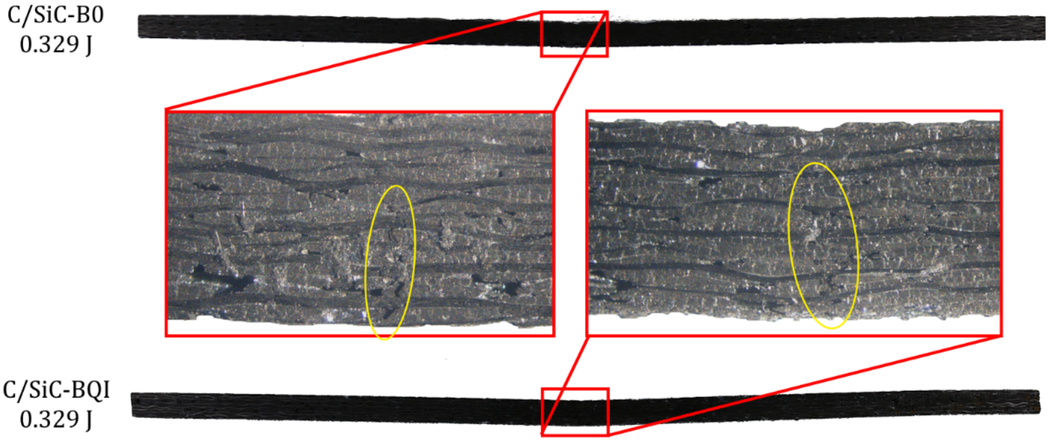

Figure 3: Permanent deflection and damage in C/SiC impacted specimens. In yellow the detail of the cracks.

All the specimens, except the one broken during the impact, were tested in three-point bending, using a span of 128 mm between the cylindrical supports, which have a diameter of $15\,mm$. An imposed velocity of $1\,mm/min$ was used. All the curves are reported in Figure 4-a for C/SiC-B0 specimens and in Figure 4-b for C/SiC-BQI specimens. In Figure 4-c the residual strength as a function of the impact energy is plotted. From the graphs, a certain threshold of tolerated impact energy for the two types of specimens can be identified, around $0.2\,J$ for C/SiC-B0 and around $0.33\,J$ for C/SiC-BQI, showing that the presence of 45° oriented plies increases considerably the toughness of the material. Moreover, even if most of the impacted specimens never reached complete failure, the post-impact flexural curves showed almost only two extreme results, a complete retention of the properties or an almost complete loss.

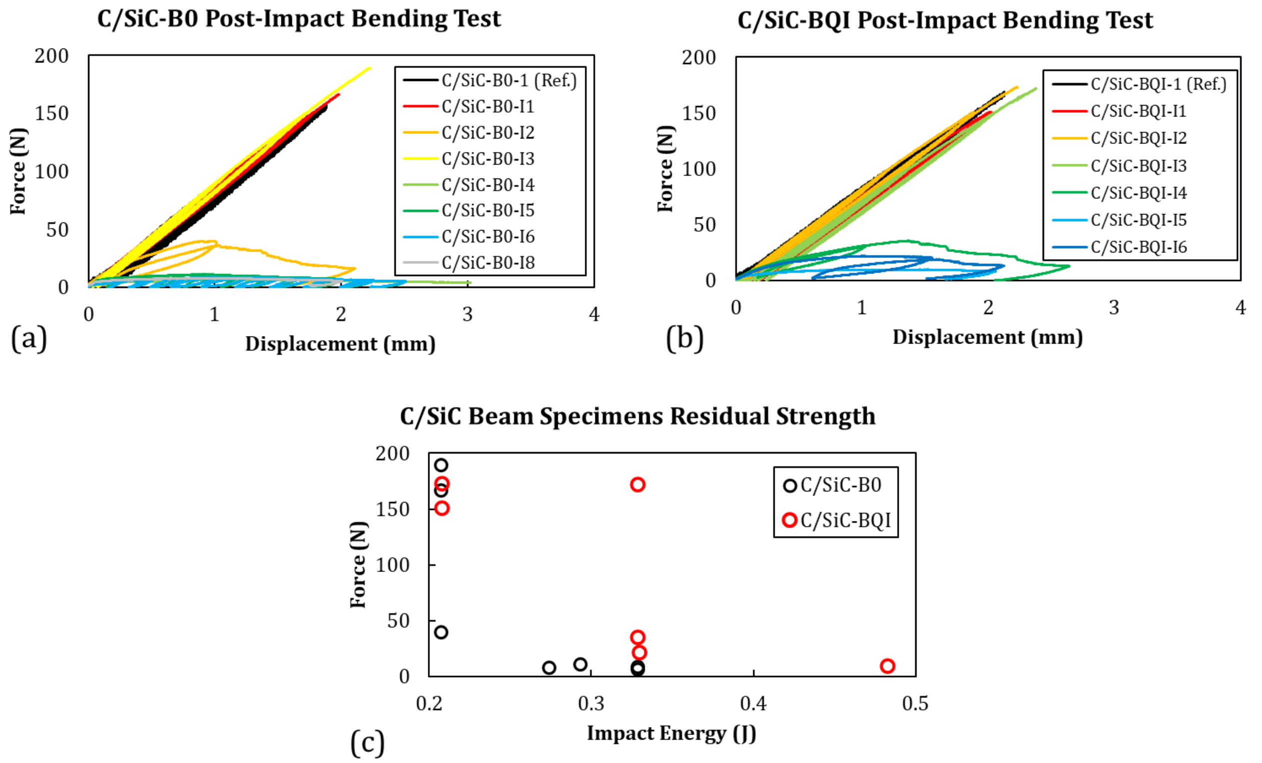

Figure 4: Post-impact bending on C/SiC beam specimens: (a) C/SiC-B0 and (b) C/SiC-BQI flexural curves, and (c) residual flexural strength as a function of impact energy.

4. Impact testing of C/SiC plates

Five C/SiC plates with dimension $150\,mm \times 100\,mm \times 4\,mm$ were impacted, while other two were used as reference for the post-impact tests. Then, three different methods were investigated for the evaluation of the residual properties of the impacted panels. First, the standard Compression After Impact (CAI) test [13] for CFRP, was attempted. Then, a flexural test was investigated, first on specimens cut out from the impacted panels and then on the entire panels. The impacted specimens, the impact energy and the after-impact test performed on each of them are reported in Table 2.

Table 2: C/SiC plate specimens used to investigate the low-energy impact resistance, the impact energies used, and the post-impact tests performed.

Specimen	Impact	Impactor mass *g*	Impact energy *J*	Indentation	CAI	Cut out bending	Entire plate bending
C/SiC-P1	-	-	-	-	yes	-	-
C/SiC-P2	yes	66	2.31	Barely visible	yes	-	-
C/SiC-P3	yes	534	2.94	yes	yes	-	-
C/SiC-P4	yes	534	8.71	yes	yes	-	-
C/SiC-P5	yes	534	2.14	Barely visible	-	yes	-
C/SiC-P6	-	-	-	-	-	-	yes
C/SiC-P7	Yes	534	2.08	Barely visible	-	-	yes

The impact energies employed were of an order of magnitude greater than those used for the beam specimens. To achieve this, the previously described rod-shaped impactor was utilized. Various drop heights were employed to adjust the impact energy of the impactor. In this case, multiple impacts could not be avoided. However, analysis of high-speed images indicated that most visible damage occurred during the initial impact. A sequence of frames from a high-speed video of an impact test on a C/SiC plate specimen is shown in Figure 5.

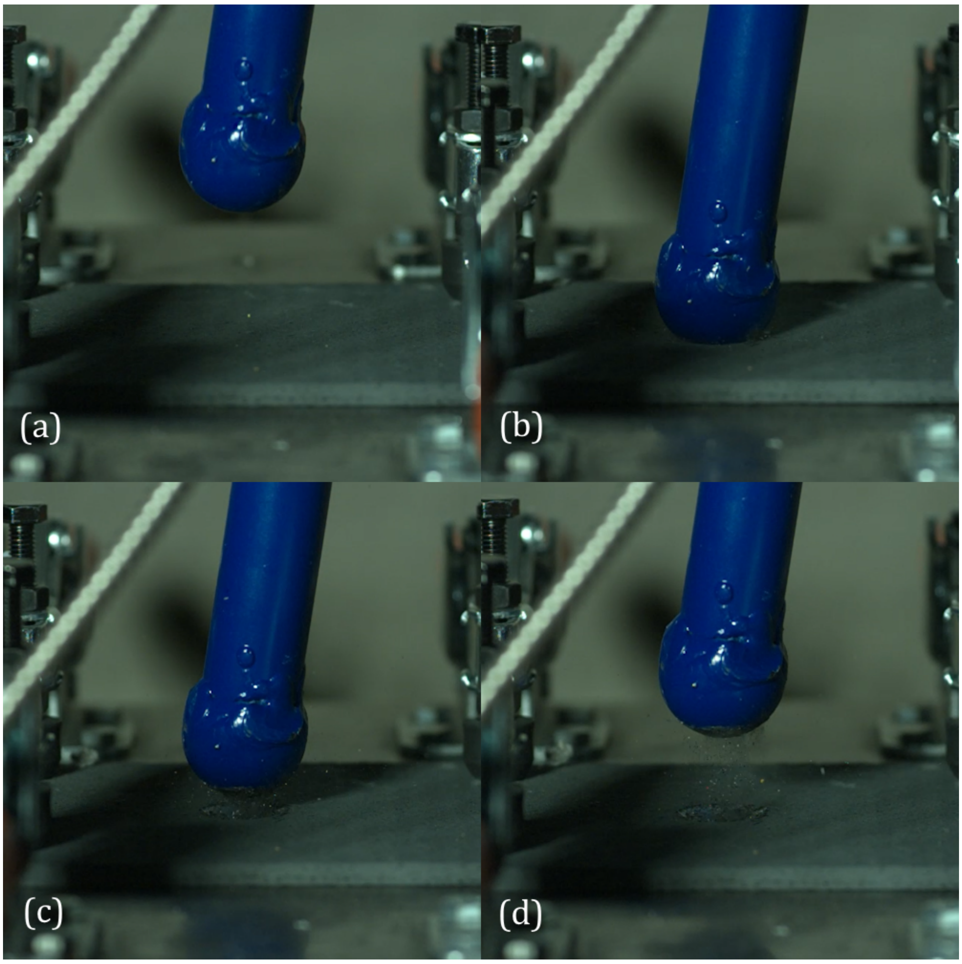

Figure 5: Frames from a high-speed video of a low-energy impact on a C/SiC plate specimen.

The panels showed to be able to tolerate a considerable amount of damage without being penetrated. The test on specimen P2 allowed us to determine the Barely Visible Impact Damage (BVID) energy of the specimens, which is between 2.0 *J* and 2.5 *J*. When this energy threshold is exceeded, an indentation with the shape of a spherical cap was typically observed on the impacted side, while a cross-shaped crack oriented along the ±45° axes was observed on the opposite side. Two exemplificative cases of the damage morphologies observed are shown in Figure 6.

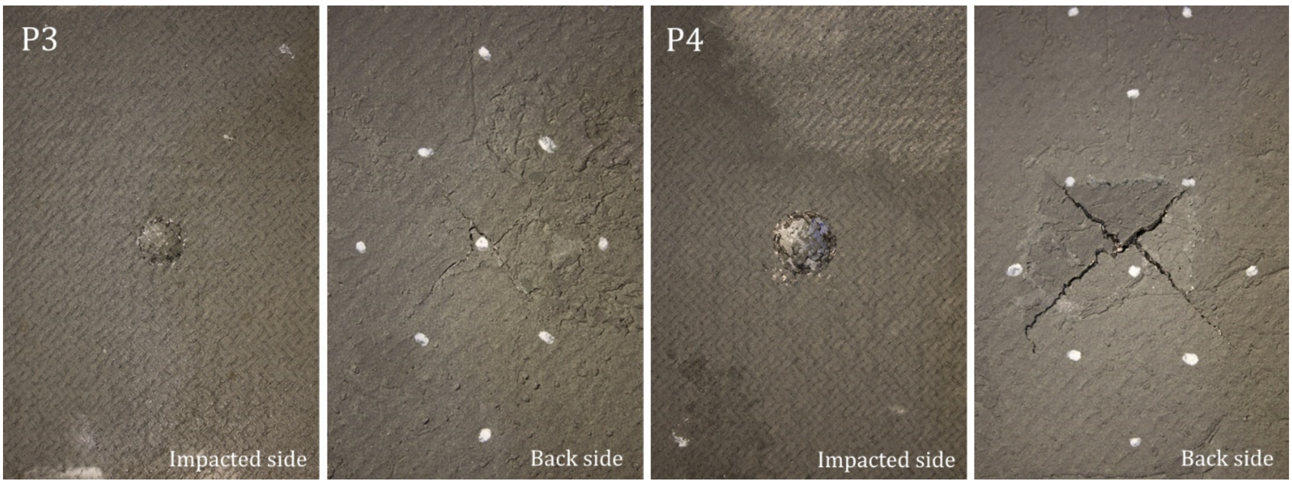

Figure 6: Exemplificative damage morphology of C/SiC plate specimens subjected to low-energy impact test.

5. Residual strength assessment

5.1 Compression After Impact

The residual properties of the impacted panels were firstly assessed performing a CAI test. The specimens were inserted in a thick steel frame which can impose an in-plane compressive load, avoiding the global instabilization, by means of two rails on the lateral sides. This test is particularly effective for impacted CFRP panels, whose delaminations could undergo blistering while compressed. For CMCs it could be less effective, considering that they better tolerate compressive loads than tensile ones, as observed in the impacted beams. Three impacted specimens were tested plus one as built, as a reference. All the four panels failed in compression, but in three of the four cases a crack opened from the top or bottom edge. This is typically related to stress concentration that forms if the specimen have small geometrical imprecisions. In the fourth one, the crack opened in the middle of the specimen, even if it did not pass through the impacted point. The CAI setup and the morphology of the cracks are shown in Figure 7.

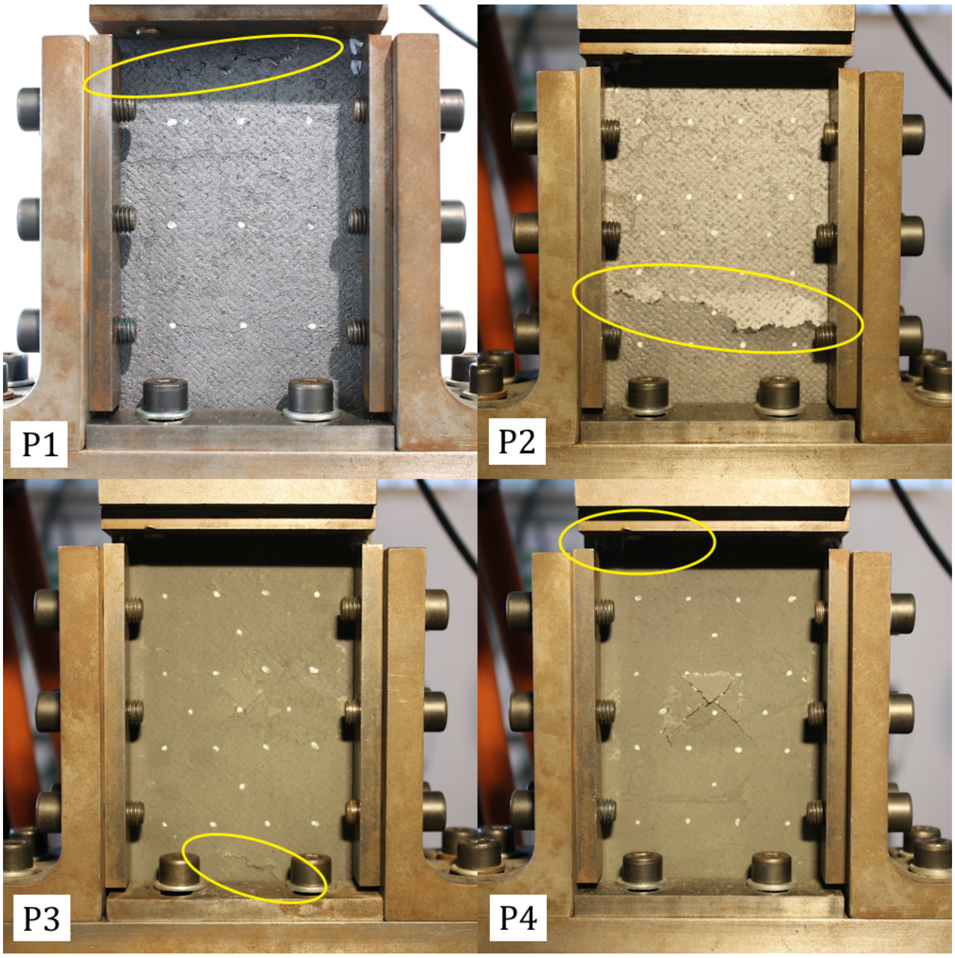

Figure 7: Compression After Impact test on C/SiC panels subjected to low-energy impacts. The yellow lines specified the cracked area.

The force/displacement curve is reported in Figure 9. The indented panels showed a reduction in strength of about 30% compared to the reference test and to the BVID one. Nonetheless, this technique showed to be not very effective for C/SiC which is particularly resistant to compression, and the failure was never triggered by the impact damage.

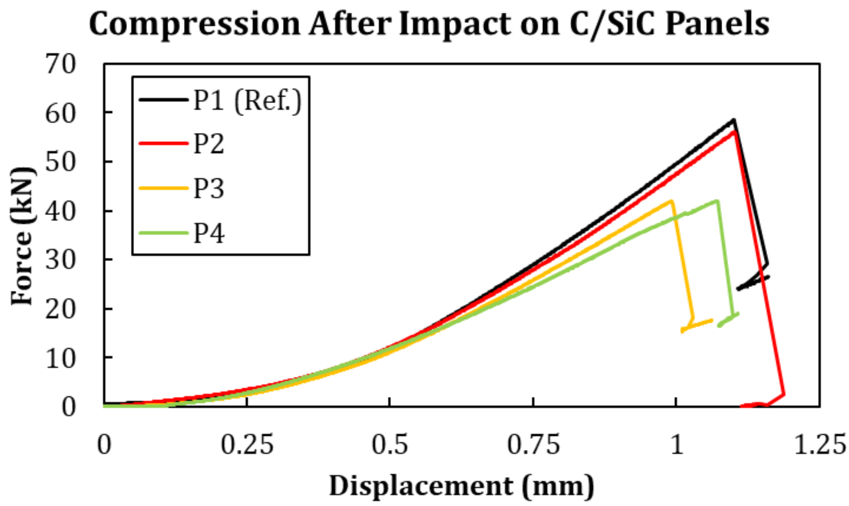

Figure 8: Force/displacement curves of Compression After Impact test of impacted C/SiC plates.

5.2 Flexural test of cut specimens

The effectiveness of three-point bending flexural testing was then investigated. The P5 specimen was impacted using the same BVID energy, determined in the test on P2 specimen. Also in this case, the indentation caused by the impactor was barely visible, as can be observed in Figure 9-a. For the first attempt, five specimens were cut out from the impacted panel as shown in Figure 9-b, thus obtaining five beam-shaped specimens, 20 *mm* wide and 150 *mm* long. They were cut such that the third specimen completely included the impacted area. This choice allowed us to compute a precise Computed Tomography (CT) scan analysis of the impacted area to evaluate the presence of internal damage developed during the impact, which would not be possible on the entire panel.

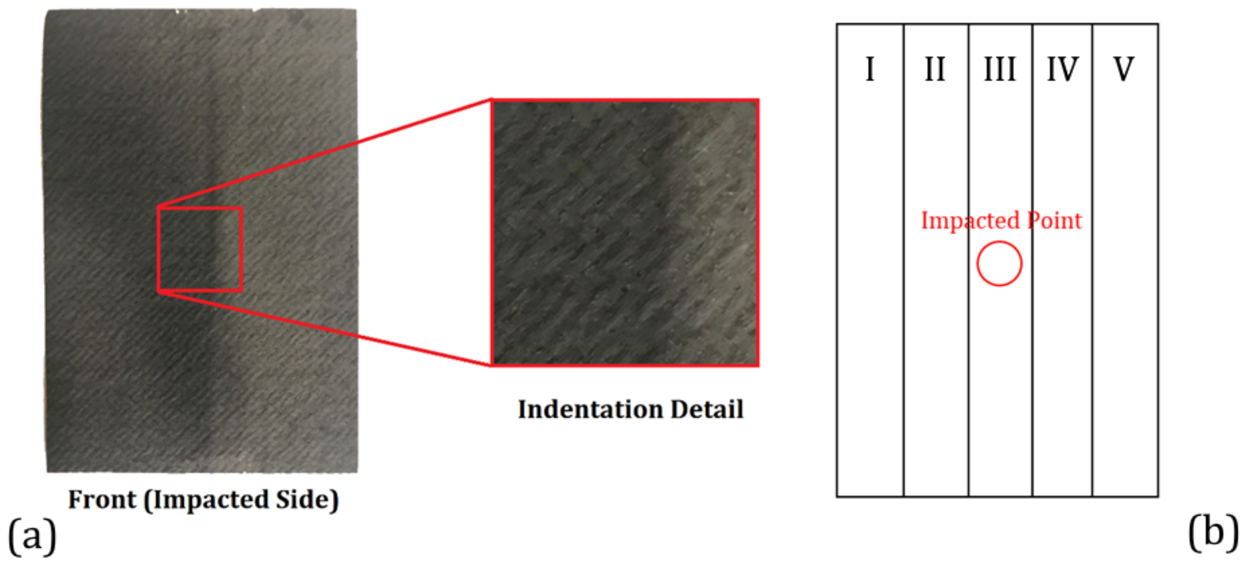

Figure 9: Impacted C/SiC panel P5: (a) detail of the Barely Visible Impact Damage and (b) cut scheme for residual properties testing.

The result of the CT scan analysis of the C/SiC-P5_III specimens are shown in Figure 10, in which three plane perspectives and a three-dimensional one are presented. In Figure 10-c, the circular-shaped indentation caused by the impactor can be observed, while in Figure 10-a and -b a series of delaminations through the thickness, marked in yellow, can be observed, resembling the cone of delaminations described in [9], starting from the impact point and enlarging through the thickness towards the tensed side of the specimen. In Figure 10-d, the cross-shaped crack typically observed in the back side of the specimens can be noticed. The presence of this quantity of delaminations is relevant because it means that a low energy impact could cause severe and hardly detectable damage, which must be considered in the design phase.

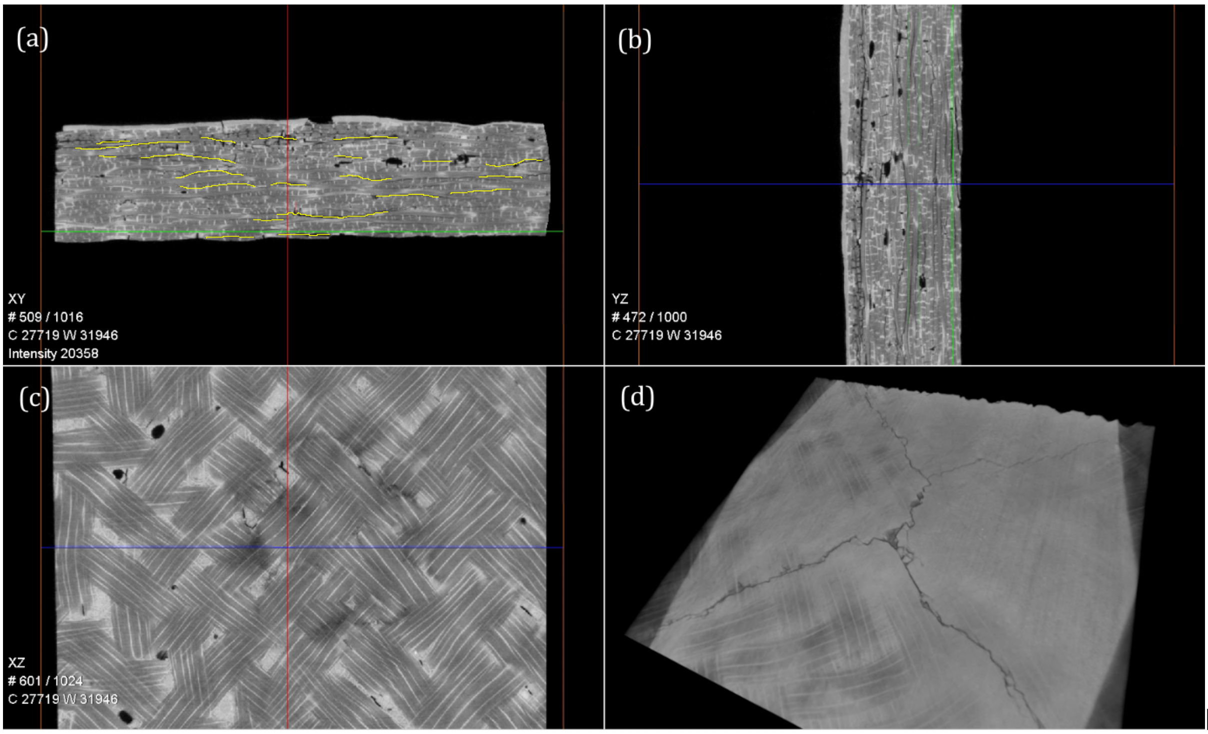

Figure 10: CT scan analysis of the impacted C/SiC panel P5.

The five specimens obtained were then tested in three-point bending, with the same test parameters used before. The specimens were positioned with the impacted face under tension, allowing for an assessment of the effect of the indentation by placing it at the point on the specimen most susceptible to fractures. In this case, the assessment of the residual properties was differential since no reference panel was cut and tested. The five curves from the five cut specimens were compared to observe the effect of the distance from the impact point, as depicted in Figure 11. These results show a reduction in flexural strength only in the central specimen, which contained the impacted region. There, the strength was reduced by more than 50%, a significant value considering the limited detectability of the damage. However, the effect of this damage is confined to a radius of less than 10 *mm*.

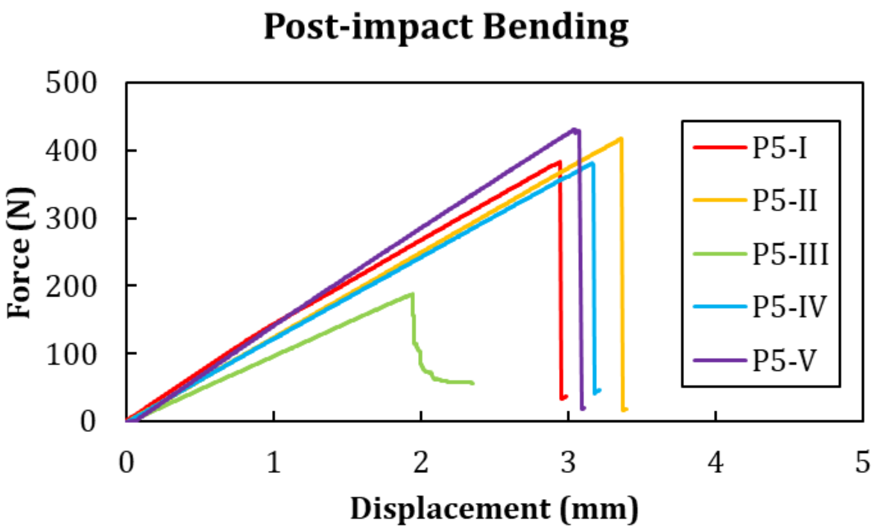

Figure 11: Flexural force/displacement curves of the five beam-shaped specimens cut from C/SiC panel specimen P5.

5.3 Flexural test of the entire plates

Cutting the impacted plates was useful to analyze the nature of the BVID. However, the reduction of the allowable values of a structure must be assessed on the entire structure, not on portions of it. For this reason, an alternative methodology was attempted, in which the entire plate is subjected to a three-point bending test to investigate the reduction of strength due to the BVID. The testing parameters are the same as the previous test, using cylinders with diameter of 25 *mm*.

Unlike a beam, when bending a plate, anticlastic curvature must be considered. This phenomenon is related to the elastic behavior of plates, wherein bending along an in-plane direction tends to develop an opposite curvature in the transversal direction, resulting in a saddle-like shape. The magnitude of this effect depends on the Poisson's ratio: the higher the Poisson's ratio, the greater the anticlastic curvature. In the case of three-point bending of a C/SiC plate, the anticlastic curvature would be opposed by the presence of the steel cylinders, causing undesired stress concentrations at the borders. Therefore, a simple FE model of the plate was used to estimate the magnitude of the anticlastic curvature. The material was modeled as perfectly elastic using the elastic properties reported in Table 3:

Table 3: Elastic properties of C/SiC used in the linear FEM model, results of previous mechanical characterization.

$E_{11} = E_{22}$	E_{33}	G_{12}	$G_{31} = G_{23}$	$\nu_{12} = \nu_{12} = \nu_{12}$
74.1 GPa	*20 GPa*	*11.4 GPa*	*3 GPa*	*0.03*

The cylinders were modeled as rigid bodies, and a Coulomb friction law was defined to replicate the interaction between the specimens and the cylinders, with a friction coefficient of 0.4. A picture of the model is shown in Figure 12-a. The results of the analysis, presented in Figure 12-b, indicated that the relative vertical displacement of the points of the section identified in Figure 12-a never exceeded 3.2%. Hence, the anticlastic curvature can be considered negligible.

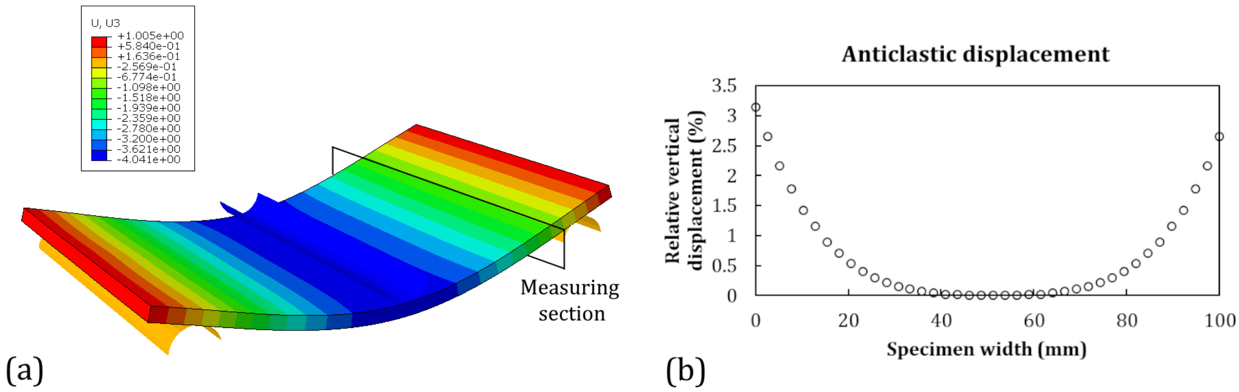

Figure 12: (a) Numerical model the flexural test of C/SiC plates and (b) the plot of the relative vertical displacement of the section which is midway between the loading cylinder and one of the supports.

Two C/SiC specimens, P6 and P7, were tested in three-point bending. The first one was tested to be used as a reference, while the second was impacted with the BVID energy before being tested. To further avoid any undesired stress concentration, elastomeric pads were placed among the C/SiC plates and the cylinders. The specimens were placed to have the impacted side subjected to tension. The experimental configuration is shown in Figure 13-a. Both the specimens failed with a fracture in the tensed face, which caused matrix cracking and fibers bridging. An example is shown in Figure 13-b. The results of the two tests are plotted in Figure 13-c, showing a clear flexural strength reduction of the panel subjected to BVID of 25% circa.

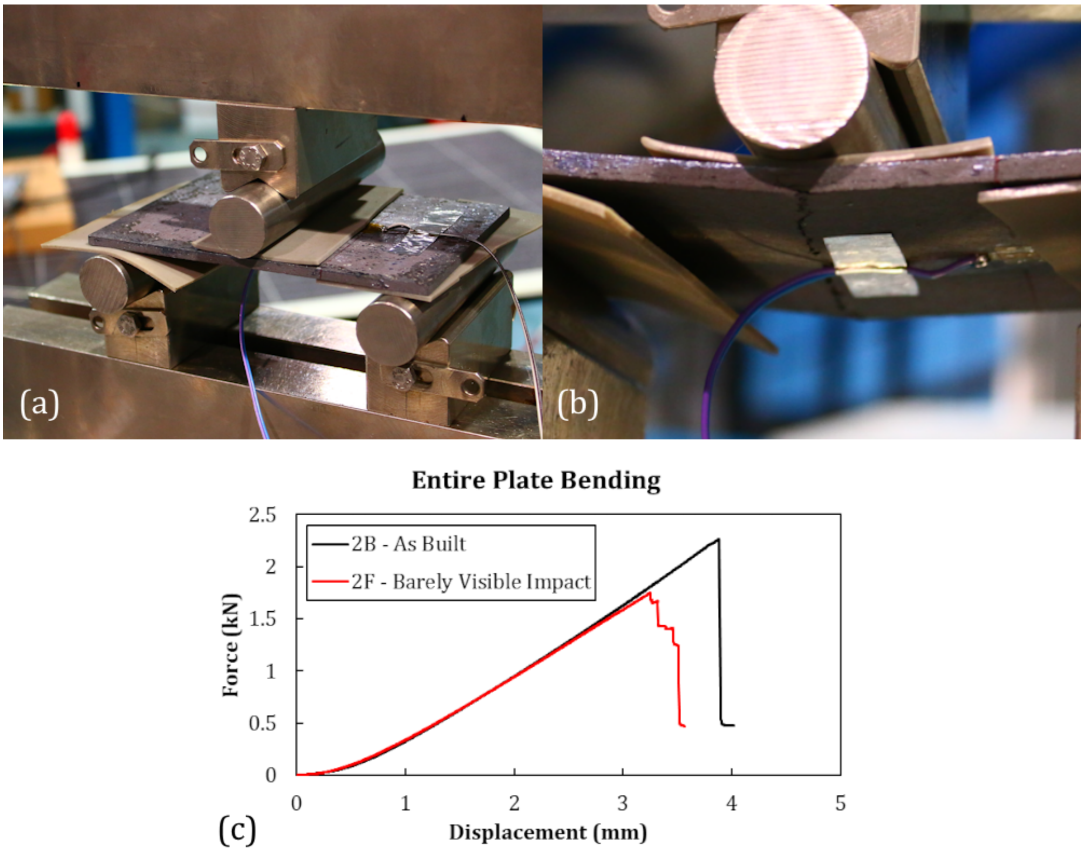

Figure 13: Three-point bending test of C/SiC panel: (a) experimental configuration, (b) fracture morphology and (c) strength comparison between as-built and impacted specimens.

6. Conclusions

In this work, a methodological study was performed to propose and assess the effectiveness of an experimental protocol to investigate the effect of low-energy impacts on LSI C/SiC panels. The scope of this method is to find the impact energy related to a Barely Visible Impact Damage (BVID) and to assess the residual properties of the panel in the presence of the BVID. With this data, C/SiC structures could be designed to resist the presence of a BVID for the time necessary before the scheduled inspections. The proposed method is composed of two tests: the first one in which the specimens were impacted to identify the BVID energy and to investigate the morphology of this damage. CT scans showed that multiple delaminations formed even if the indentation on the specimen's surface is hardly detectable. In case of higher impact energies, a sphere cap shaped indentation on the impacted side, and a cross-shaped crack along the 45° oriented axes were observed. Then, after an accurate design to avoid unwanted stress concentration, a three-point bending test was performed on the impacted panel showing a reduction of flexural strength of 25% circa in the presence of a BVID. These results identify the reduction of the allowable value of the material that must be considered during the design of C/SiC structures.

7. Aknowledgement

This work was supported by the Italian Space Agency (ASI) as part of the project AM3aC2A: Multi-scale approach for modelling CMC and UHTCMC materials.

8. Contact Author Email Address

For contacts, please mail to: antoniomariacaporale@polimi.it

9. Copyright Statement

proceedings or as individual off-prints from the proceedings.

References

[1] N. P. Bansal e J. Lamon, A c. di, *Ceramic Matrix Composites: Materials, Modeling and Technology*, 1ª ed. Wiley, 2014. doi: 10.1002/9781118832998.

[2] Federal Aviation Administration, «AC 23-13A - Fatigue, fail-safe and damage-tolerance evaluation of metallic structure for normal, utility, acrobatic and commuter category airplanes». 2005.

[3] W. Krenkel, «C/C-Sic Composites for Hot Structures and Advanced Friction Systems», in *Ceramic Engineering and Science Proceedings*, vol. 24, W. M. Kriven e H.-T. Lin, A c. di, Hoboken, NJ, USA: John Wiley & Sons, Inc., 2003, pp. 583–592. doi: 10.1002/9780470294826.ch85.

[4] W. Krenkel e F. Berndt, «C/C–SiC composites for space applications and advanced friction systems», *Materials Science and Engineering: A*, vol. 412, fasc. 1–2, pp. 177–181, dic. 2005, doi: 10.1016/j.msea.2005.08.204.

[5] W. Krenkel, «Carbon Fiber Reinforced CMC for High-Performance Structures», *Int J Applied Ceramic Tech*, vol. 1, fasc. 2, pp. 188–200, apr. 2004, doi: 10.1111/j.1744-7402.2004.tb00169.x.

[6] R. Kochendörfer e N. Lützenburger, «Applications of CMCs Made via the Liquid Silicon Infiltration (LSI) Technique», in *High Temperature Ceramic Matrix Composites*, 1ª ed., W. Krenkel, R. Naslain, e H. Schneider, A c. di, Wiley, 2001, pp. 275–287. doi: 10.1002/3527605622.ch45.

[7] D. Jiang, H. Qian, Y. Xu, D. Zhang, e J. Zheng, «Residual strength of C/SiC composite after low-velocity impact», *Materials Today Communications*, vol. 30, p. 103140, mar. 2022, doi: 10.1016/j.mtcomm.2022.103140.

[8] Y. Lin e B. Liu, «Study on Impact Resistance of C/SiC Ceramic Matrix Composites for Thermal Protection of the Aerospace Vehicle», *Mathematical Problems in Engineering*, vol. 2021, pp. 1–10, ago. 2021, doi: 10.1155/2021/6255014.

[9] H. Mei, C. Yu, Y. Xu, D. Han, e L. Cheng, «Effect of impact energy on damage resistance and mechanical property of C/SiC composites under low velocity impact», *Materials Science and Engineering: A*, vol. 687, pp. 141–147, feb. 2017, doi: 10.1016/j.msea.2017.01.062.

[10] A. M. Caporale, P. Galizia, B. Zanardi, A. Vinci, D. Sciti, e A. Airoldi, «A bi-phasic numerical approach for non-linear response and stiffness recovery related to residual thermal stress in UHTCMCs», *Journal of the European Ceramic Society*, p. S0955221924002565, mar. 2024, doi: 10.1016/j.jeurceramsoc.2024.03.038.

[11] M. Riva, A. Airoldi, A. M. Caporale, L. Cavalli, e M. De Stefano Fumo, «Interlaminar Response of LSI-Produced C/SiC Ceramic Matrix Composites: Experiments and Modelling», *Composites Part A: Applied Science and Manufacturing*, vol. 175, p. 107774, dic. 2023, doi: 10.1016/j.compositesa.2023.107774.

[12] «Standard Test Method for Measuring the Damage Resistance of a Fiber-Reinforced Polymer Matrix Composite to a Drop-Weight Impact Event», ASTM, D7136.

[13] «Standard Test Method for Compressive Residual Strength Properties of Damaged Polymer Matrix Composite Plates», ASTM, D7137.